Compact and high conversion efficiency mode sorting asymmetric Y junction using shortcuts to adiabaticity

S. Martínez-Garaot[1], Shuo-Yen Tseng[2,3,*], J. G. Muga[1,4]

[1] *Departamento de Química Física, UPV/EHU, Apdo. 644, 48080 Bilbao, Spain*
[2] *Department of Photonics, National Cheng Kung University, Tainan 701, Taiwan*
[3] *Advanced Optoelectronic Technology Center, National Cheng Kung University, Tainan 701, Taiwan*
[4] *Department of Physics, Shanghai University, 200444 Shanghai, People's Republic of China*
[*] *Corresponding author: tsengsy@mail.ncku.edu*

Compiled February 20, 2014

We propose a compact and high conversion efficiency asymmetric Y junction mode multiplexer/demultiplexer for applications in on-chip mode-division multiplexing (MDM). Traditionally, mode-sorting is achieved by adiabatically separating the arms of a Y junction. We shorten the device length using invariant-based inverse engineering and achieve better conversion efficiency than the adiabatic device. © 2014 Optical Society of America

OCIS codes: 000.1600, 200.4650, 060.4230, 130.3120.

As optical communications over single-mode optical waveguides are fast approaching their capacity limits, using multiple spatial modes in optical transmission systems to increase information capacity has attracted lots of attention [1,2]. In mode-division multiplexing (MDM) systems [3], the multiple propagating modes in the system provide the extra degrees of freedom for potential capacity increase. However, to avoid intermodal dispersion, one needs to be able to excite and detect the spatial modes independently in MDM systems. So far, most of the efforts for the multiplexing/demultiplexing in MDM systems are focused on fiber based systems, but there is also interest in realizing integrated multimode systems [4–6]. In integrated optical waveguides, the asymmetric Y junction can be designed to function as a mode sorter [7–9]. The asymmetric Y junction has a two-modes stem and two diverging single-mode arms with different widths. When the fundamental (second) mode of the stem propagates though the junction, it evolves into the fundamental mode of the wider (narrower) output arm, and vice versa. The mode sorting behavior can be attributed to the fact that a mode would evolve into the mode of the output arm with the closest effective index [7]. However, this smooth evolution can only occur when the variation at the junction is slow enough such that the evolution is adiabatic, reducing the coupling between the local eigenmodes (supermodes) of the structure. However, the adiabatic criterion often leads to a small branching angle between the arms and thus a long device length to achieve the desired arm separation. The challenge in integrated mode sorting Y junction multiplexer/demultiplexer design is thus to reduce the device lengths while minimizing the crosstalk between the arms.

So far, the efforts have been focused on optimizing the device length without violating the adiabatic criterion [10]. There have also been attempts to find the optimal shape function that minimizes the coupling between the supermodes [11]. These approaches are based on the adiabatic approximation, and a well-known criterion for mode sorting operation of the asymmetric Y junction is given by the mode conversion factor (MCF) as [7]:

$$\mathrm{MCF} = \frac{|\beta_A - \beta_B|}{\theta \gamma_{AB}}, \tag{1}$$

where θ is the branching angle of the Y junction arms, β_A and β_B are the propagation constants of the modes supported by single mode arms A and B, and $\gamma_{AB} = 0.5\sqrt{(\beta_A + \beta_B)^2 - (2k_0 n)^2}$ with n the cladding refractive index and k_0 the free-space wavenumber. When the MCF is larger (smaller) than 0.43, an asymmetric Y junction acts as a mode sorter (power divider). For a given material system n, branching waveguides dimensions β_A and β_B, and branch separation D, the required device length $L = D/\theta$ is limited by θ obtained from Eq. (1). Moreover, as long as there is finite coupling between the supermodes in the adiabatic evolution, the conversion efficiency will only be unity at specific operating points [12, 13].

Recently, many coherent quantum phenomena have been exploited to implement light manipulation in waveguide structures based on the analogies between quantum mechanics and wave optics [14]. At the same time, the development in new ways to manipulate quantum systems with high-fidelity and in a short interaction time using "shortcuts to adiabaticity" [15] has inspired the design of a family of novel coupled-wave devices [16–21]. In particular, the invariant-based inverse-engineering approach [22–24] provides a versatile tool for the design of fast and robust waveguide couplers [19], in which the system dynamics are described using the eigenstates of the invariant $\mathbf{I}$ corresponding to the system Hamiltonian $\mathbf{H}$. While previous works [16, 17, 20, 21] focused on grating-assisted mode conversion in multimode waveguides, in this letter, we apply the shortcut to adiabaticity to design short asymmetric Y junction mode

multiplexer/demultiplexer beyond the adiabatic limit.

We consider the asymmetric Y junction shown schematically in Fig. 1, in which a two-modes stem waveguide evolves to two single-mode waveguides A (wider) and B (narrower) in a length L. The evolution of the fundamental modal amplitudes in waveguides A and B can be described by the coupled mode equations as

$$\frac{d}{dz}\begin{bmatrix} A \\ B \end{bmatrix} = -i\begin{bmatrix} \lambda(z) & -\delta(z) \\ -\delta(z) & -\lambda(z) \end{bmatrix}\begin{bmatrix} A \\ B \end{bmatrix} = -i\mathbf{H}\begin{bmatrix} A \\ B \end{bmatrix}, \tag{2}$$

where δ (real) is the coupling coefficient, and $\lambda = (\beta_B - \beta_A)/2$ describes the mismatch. For the two-modes stem waveguide at $z = 0$, $\lambda(0) = 0$ and $\delta(0) = \omega_0$. Solving for the eigenvectors of $\mathbf{H}$, we find two adiabatic supermodes, $|a_A\rangle = \sin\alpha|\Psi_1\rangle + \cos\alpha|\Psi_2\rangle$ and $|a_B\rangle = \cos\alpha|\Psi_1\rangle - \sin\alpha|\Psi_2\rangle$, where $|\Psi_1\rangle \equiv \binom{0}{1}$, $|\Psi_2\rangle \equiv \binom{1}{0}$, and $\alpha = (1/2)\tan^{-1}(\delta/\lambda)$. λ and δ are related to the branch geometry, which is yet to be specified. We impose the boundary conditions

$$\delta(0) = \omega_0, \lambda(0) = 0, \delta(L) = 0, \lambda(L) = \lambda_L, \tag{3}$$

such that the structure corresponds to a two-modes stem waveguide at $z = 0$ and two single-mode waveguides at $z = L$. For the conventional adiabatic Y junction design, the goal is to design the evolution of λ and δ through device geometry such that the coupling between $|a_A\rangle$ and $|a_B\rangle$ are minimized. When the adiabatic criterion is not satisfied, and there is finite coupling between $|a_A\rangle$ and $|a_B\rangle$, the mode sorting performance will deteriorate. In the following, we use the invariant-based inverse engineering approach to design a protocol in which the mode sorting is achieved at a shorter length than required by the adiabatic criterion.

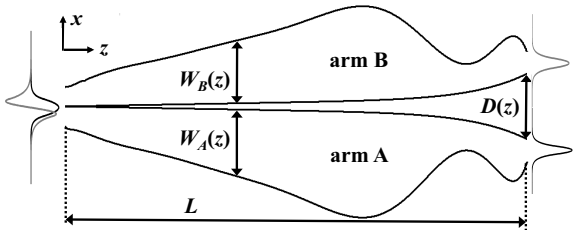

Fig. 1. Schematic of the asymmetric Y junction.

Replacing the spatial variation z with the temporal variation t, Eq. (2) is equivalent to the time-dependent Schrödinger equation ($\hbar = 1$) describing the interaction dynamics of a two-state system, and $\mathbf{H}$ is the Hamiltonian. Associated with $\mathbf{H}$ there are Hermitian dynamical invariants $\mathbf{I}(t)$, fulfilling $\partial_t\mathbf{I} + (1/i)[\mathbf{I}, \mathbf{H}] = 0$, so that their expectation values remain constant. $\mathbf{I}$ can be written as (where t is replaced by z and hereafter) [22]

$$\mathbf{I}(z) = \frac{1}{2}\begin{pmatrix} \cos\theta & \sin\theta e^{i\varphi} \\ \sin\theta e^{-i\varphi} & -\cos\theta \end{pmatrix}, \tag{4}$$

where $\theta \equiv \theta(z)$ and $\varphi \equiv \varphi(z)$ are z-dependent angles. The eigenstates of the invariant $\mathbf{I}(z)$ satisfy $\mathbf{I}(z)|\phi_n(z)\rangle = \lambda_n|\phi_n(z)\rangle$, and they can be written as

$$|\phi_+(z)\rangle = \begin{pmatrix} \cos\frac{\theta}{2}e^{-i\varphi} \\ \sin\frac{\theta}{2} \end{pmatrix}, |\phi_-(z)\rangle = \begin{pmatrix} \sin\frac{\theta}{2} \\ -\cos\frac{\theta}{2}e^{i\varphi} \end{pmatrix}. \tag{5}$$

An invariant $\mathbf{I}(z)$ of $\mathbf{H}(z)$ satisfies $i\hbar\partial_z(\mathbf{I}(z)|\Psi(z)\rangle) = \mathbf{H}(z)(\mathbf{I}(z)|\Psi(z)\rangle)$ [25]. According to Lewis-Riesenfeld theory, the system state can be written as $|\Psi(z)\rangle = \Sigma_n c_n e^{i\gamma_n(z)}|\phi_n(z)\rangle$, where the c_n are time-independent amplitudes, and the $\gamma_n(z)$ are Lewis-Riesenfeld phases. The time independent c_n implies that the system state will follow the eigenstate of the invariant exactly without mutual coupling. To engineer the Hamiltonian $\mathbf{H}$ such that the mode sorting is exact, we design the invariant first and then obtain the Hamiltonian from it. Applying the boundary condition $[\mathbf{H}(z), \mathbf{I}(z)] = 0$ at $z = 0$ and $z = L$ such that the eigenvectors of $\mathbf{H}(z)$ and $\mathbf{I}(z)$ coincide at the input and output, the invariant will drive the input eigenstates of $\mathbf{H}$ to the output eigenstates of $\mathbf{H}$ exactly. Using the invariance condition, we find

$$\delta(z) = -\dot{\theta}(z)/\sin\varphi(z), \tag{6}$$

$$\lambda(z) = -\delta(z)\cot\theta(z)\cos\phi(z) - \dot{\varphi}(z). \tag{7}$$

Using the commutativity of $\mathbf{H}(z)$ and $\mathbf{I}(z)$ at the input and output and Eq. (3), we obtain

$$\theta(0) = \pi/2, \varphi(0) = \pi, \theta(L) = \pi, \dot{\theta}(L) = 0. \tag{8}$$

These conditions lead to indeterminacies in Eqs. (6) and (7), so we apply l'Hôpital's rule repeatedly and find the additional boundary conditions [24]

$$\dot{\theta}(0) = \ddot{\theta}(0) = \dot{\varphi}(0) = 0, \dddot{\theta}(0) = -\omega_0\dot{\lambda}(0), \tag{9}$$
$$\ddot{\varphi}(0) = -\dot{\lambda}(0), \varphi(L) = \pi/2, \dot{\varphi}(L) = -\lambda_L/3,$$

with $\dot{\lambda}(0) \neq 0$. With the boundary conditions in Eq. (9), the evolution of the invariant parameters $\theta(z)$ and $\varphi(z)$ can be obtained through interpolation assuming a polynomial ansatz [24]. Then the Hamiltonian functions δ and λ can be obtained from Eqs. (6) and (7). We finally use the simplex-based mapping method described in [24] to map the designed Hamiltonian to a realizable waveguide geometry. Device performance will be related to the choice of interpolation ansatz. It is beyond the scope of this letter to categorize or evaluate the various ansatz that are possible; rather, we focus on the polynomial ansatz to demonstrate the device concept.

Now, we illustrate the design of a compact mode sorting asymmetric Y junction in a conventional planar integrated optics platform and perform beam propagation method (BPM) simulations to verify the designs. The scalar 2D BPM code used in the simulations solves the scalar and paraxial wave equation using the finite difference scheme with the transparent boundary condition. We choose a polymer channel waveguide structure for beam propagation simulations. The design parameters

are chosen as follows: 3 μm thick SiO_2 (n =1.46) on a Si (n = 3.48) wafer is used for the bottom cladding layer, the core consists of a 2.4 μm layer of BCB (n = 1.53), and the upper cladding is epoxy (n = 1.50). The device is simulated at 1.55 μm input wavelength and the TE polarization. Subsequent analysis are performed on the 2D structure obtained using the effective index method. For the Y junction input and outputs, we choose a input stem waveguide width of 5.8 μm supporting two modes, and the output single mode waveguides widths are $W_A(L)$=3.5 μm and $W_B(L)$=3.29 μm. We target a final waveguide separation $D(L)$ of 10 μm so that the coupling between the output branches is negligible. Substituting the corresponding waveguide parameters into Eq. (1), MCF=$0.1277/\theta$ (with θ in degrees) indicating the device is a mode sorter for $\theta < 0.3°$. For a conventional linearly separating adiabatic Y junction, this corresponds to a device length of larger than 2 mm to achieve a final separation $D(L)$ of 10 μm. In Fig. 2, we show the simulated fractional power in the fundamental modes (conversion efficiency) of waveguides A and B using the second mode as the input for different device lengths. When the device length is greater than 10 mm, the mode sorting characteristics is well established. The transition from power divider to mode sorter at around 2 mm predicted by MCF calculations is also evident. We also observe that the conversion efficiency starts to fall and will oscillate when the length keeps increasing beyond 10 mm, as a result of finite coupling between the supermodes [11].

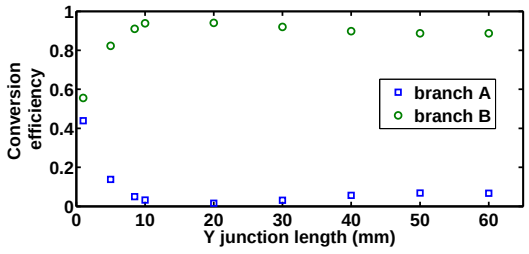

Fig. 2. Conversion efficiencies of a linearly separating Y junction using the second mode as the input for different device lengths

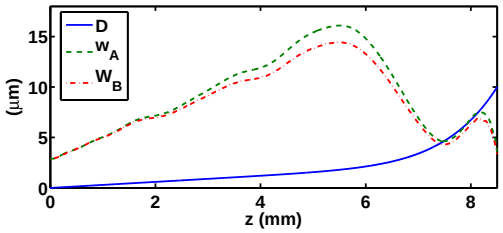

Fig. 3. Parameters for the invariant based Y junction.

For the invariant based design, the boundary conditions in Eq. (3) are fixed by the waveguide parameters at the device input and output. To map the Hamiltonian to the waveguide parameters of the Y junction, we choose the widths of waveguides $W_A(z)$ and $W_B(z)$ and the separation $D(z)$ shown in Fig. 1 as the free parameters in the simplex search. The resulting parameters are shown in Fig. 3 for a L = 8.5 mm device. The corresponding Y junction geometry is shown in Fig. 4. In Fig. 4(a), the BPM results show that the fundamental mode has evolved to waveguide A at the output. And the evolution of the second mode to waveguide B is shown in Fig. 4(b). We also show the BPM results for the linearly separating adiabatic Y junction of the same length in Fig. 5. In Fig. 6, we compare the output field of the invariant-based mode sorter and the linear mode sorter, both at a length of 8.5 mm. The conversion efficiency of the invariant based design is calculated to be 0.98 for both modes while the linearly separating design is 0.92 for both modes. The insertion loss of the invariant based design are 0.267 dB and 0.185 dB for the fundamental and the second modes, respectively; and 0.481 dB and 0.604 dB for the linearly separating design. The higher insertion loss of the linearly separating design can be attributed to coupling into the radiation modes. On the other hand, the evolution of the invariant based design should follow the eigenstates of the invariant exactly without coupling into the radiation modes. The observed loss can be attributed to small coupling into the radiation modes, because the ideal protocol is only approximately mapped to the coordinate space model in the simplex-based mapping [24]. This also results in the conversion efficiency being less than 1. Although the width of the invariant based design is larger than the linearly separating design, we note from Fig. 2 that the conversion efficiency of the linearly separating design would not reach 0.98 even when the length of the junction is increased to 60 mm. As a result, the invariant based design can achieve high conversion efficiency with a more compact device footprint. The fabrication tolerance is studied by adding width variations δW to W_A and W_B while keeping D unchanged in the simulations. The resulting conversion efficiencies for different δW using the

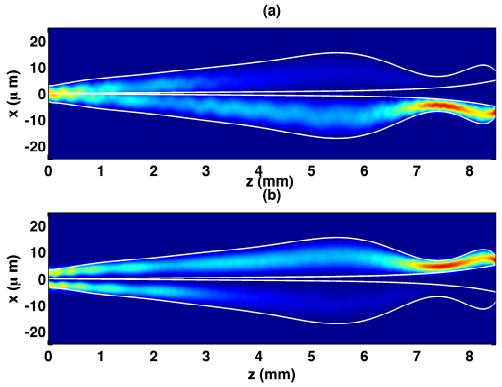

Fig. 4. Mode sorting operation of the invariant based Y junction. Input (a) fundamental mode (b) second mode.

second mode as the input is shown in Fig. 7, indicating that the proposed device has a large fabrication tolerance better than 1000 nm.

In conclusion, we demonstrated that the invariant-based inverse engineering approach can be applied successfully to asymmetric Y junction design. By describing the system dynamics using the dynamical invariants, the system evolution can be engineered to achieve mode sorting in a short distance. The compact design exhibits a higher conversion efficiency than the conventional adiabatic design at a shorter device length.

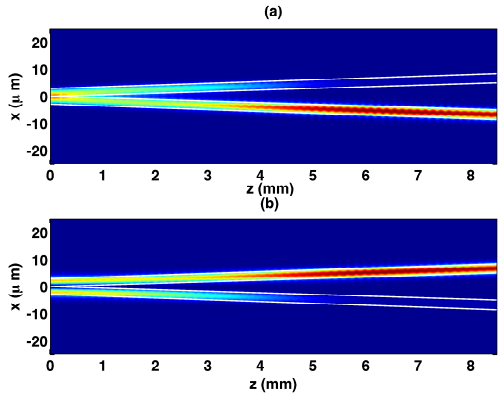

Fig. 5. Mode sorting operation of the linearly separating Y junction. Input (a) fundamental mode (b) second mode.

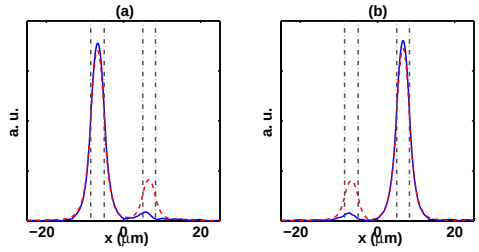

Fig. 6. Output field profile of the Y junctions. Solid: invariant based. Dashed: linearly separating. Dash-dotted: waveguide walls. Input (a) fundamental mode (b) second mode.

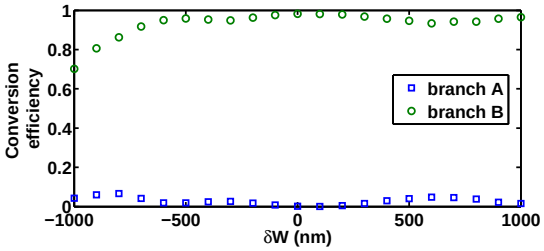

Fig. 7. Conversion efficiencies as a function of width variation using the second mode as the input.

Acknowledgement

This work was supported by the National Science Council of Taiwan (Grant No. NSC 100-2221-E-006-176-MY3), the Basque Country Government (Grant No. IT472-10), Ministerio de Economía y Competitividad (Grant No. FIS2012-36673-C03-01), and the program UFI 11/55. S. M.-G. acknowledges a fellowship by UPV/EHU.

References

1. H. R. Stuart, Science **289**, 281 (2000).
2. J. Wang, J.-Y. Yang, I. M. Fazal, N. Ahmed, Y. Yan, H. Huang, Y. Ren, Y. Yue, S. Dolinar, M. Tur, and A. E. Wilner, Nat. Photon. **6**, 488 (2012).
3. S. Berdagué and P. Facq, Appl. Opt. **21**, 1950 (1982).
4. V. Liu, D. A. B. Miller, and S. Fan, Opt. Express **20**, 28388 (2012).
5. W. Chen, P. Wang, and J. Yang, Opt. Express **21**, 25113 (2013).
6. J. B. Driscoll, R. R. Grote, B. Souhan, J. I. Dadap, M. Lu, and R. M. Osgood, Opt. Lett. **38**, 1854 (2013).
7. W. K. Burns and A. F. Milton, IEEE J. Quantum Electron. **11**, 32 (1975).
8. J. D. Love and N. Riesen, J. Lightw. Technol. **30**, 304 (2012).
9. N. Riesen and J. D. Love, Appl. Opt. **51**, 2778 (2012).
10. J. D. Love, R. W. C. Vance, and A. Joblin, Opt. Quantum. Electron. **28**, 353 (1996).
11. X. Sun, H.-C. Liu, and A. Yariv, Opt. Lett. **34,** 280 (2009).
12. R. R. A. Syms, IEEE Photon. Technol. Lett. **4,** 1135 (1992).
13. G. T. Paloczi, A. Eyal, and A. Yariv, IEEE Photon. Technol. Lett. **16,** 515 (2004).
14. S. Longhi, Laser and Photon. Rev. **3,** 243 (2009).
15. E. Torrontegui, S. Ibáñez, S. Martínez-Garaot, M. Modugno, A. del Campo, D. Guéry-Odelin, A. Ruschhaupt, X. Chen, and J. G. Muga, Adv. At. Mol. Opt. Phys. **62,** 117 (2013).
16. S.-Y. Tseng and X. Chen, Opt. Lett. **37,** 5118 (2012).
17. T.-Y. Lin, F.-C. Hsiao, Y.-W. Jhang, C. Hu, and S.-Y. Tseng, Opt. Express **20,** 24085 (2012).
18. S.-Y. Tseng, Opt. Express **21**, 21224 (2013).
19. S.-Y. Tseng and Y.-W. Jhang, IEEE Photon. Technol. Lett. **25**, 2478 (2013).
20. C.-S. Yeih, H.-X. Cao, and S.-Y. Tseng, IEEE Photon. Technol. Lett. **26**, 123 (2014).
21. K.-H. Chien, C.-S. Yeih, and S.-Y. Tseng, J. Lightw. Technol. **31**, 3387 (2013).
22. X. Chen, E. Torrontegui, and J. G. Muga, Phys. Rev. A **83,** 062116 (2011).
23. X. Chen and J. G. Muga, Phys. Rev. A **86**, 033405 (2012).
24. S. Martínez-Garaot, E. Torrontegui, X. Chen, M. Modugno, D. D. Guéry-Odelin, S.-Y. Tseng, and J. G. Muga, Phys. Rev. Lett. **111**, 213001 (2013).
25. H. R. Lewis and W. B. Riesenfeld, J. Math. Phys. **10,** 1458 (1969).

Informational Fifth Page

References

1. H. R. Stuart, "Dispersive multiplexing in multimode optical fiber," Science **289**, 281283 (2000).
2. J. Wang, J.-Y. Yang, I. M. Fazal, N. Ahmed, Y. Yan, H. Huang, Y. Ren, Y. Yue, S. Dolinar, M. Tur, and A. E. Wilner, "Terabit free-space data transmission employing orbital angular momentum multiplexing," Nat. Photon. **6**, 488-496 (2012).
3. S. Berdagué and P. Facq, "Mode division multiplexing in optical fibers," Appl. Opt. **21**, 1950-1955 (1982).
4. V. Liu, D. A. B. Miller, and S. Fan, "Ultra-compact photonics crystal waveguide spatial mode converter and its connection to the optical diode effect," Opt. Express **20**, 28388-28397 (2012).
5. W. Chen, P. Wang, and J. Yang, "Mode multi/demultiplexer based on cascaded asymmetric Y-junctions," Opt. Express **21**, 25113-25119 (2013).
6. J. B. Driscoll, R. R. Grote, B. Souhan, J. I. Dadap, M. Lu, and R. M. Osgood, "Asymmetric Y junctions in silicon waveguides for on-chip mode-division multiplexing," Opt. Lett. **38**, 1854-1856 (2013).
7. W. K. Burns and A. F. Milton, "Mode conversion in planar-dielectric separating waveguides," IEEE J. Quantum Electron. **11**, 32-39 (1975).
8. J. D. Love and N. Riesen, "Single, few-, and multimode Y-junctions," J. Lightw. Technol. **30**, 304-309 (2012).
9. N. Riesen and J. D. Love, "Design of mode-sorting asymmetric Y-junctions," Appl. Opt. **51**, 2778-2783 (2012).
10. J. D. Love, R. W. C. Vance, and A. Joblin, "Asymmetric, adiabatic multipronged planar splitters," Opt. Quantum. Electron. **28**, 353-369 (1996).
11. X. Sun, H.-C. Liu, and A. Yariv, "Adiabaticity criterion and the shortest adiabatic mode transformer in a coupled-waveguide system," Opt. Lett. **34,** 280-282 (2009).
12. R. R. A. Syms, "The digital directional coupler: improved design," IEEE Photon. Technol. Lett. **4,** 1135-1138 (1992).
13. G. T. Paloczi, A. Eyal, and A. Yariv, "Wavelength-insensitive nonadiabatic mode evolution couplers," IEEE Photon. Technol. Lett. **16,** 515-517 (2004).
14. S. Longhi, "Quantum-optical analogies using photonic structures," Laser and Photon. Rev. **3,** 243-261 (2009).
15. E. Torrontegui, S. Ibáñez, S. Martínez-Garaot, M. Modugno, A. del Campo, D. Guéry-Odelin, A. Ruschhaupt, X. Chen, and J. G. Muga, "Shortcuts to adiabaticity," Adv. At. Mol. Opt. Phys. **62,** 117-169 (2013).
16. S.-Y. Tseng and X. Chen, "Engineering of fast mode conversion in multimode waveguides," Opt. Lett. **37,** 5118-5120 (2012).
17. T.-Y. Lin, F.-C. Hsiao, Y.-W. Jhang, C. Hu, and S.-Y. Tseng, "Mode conversion using optical analogy of shortcut to adiabatic passage in engineered multimode waveguides," Opt. Express **20,** 24085-24092 (2012).
18. S.-Y. Tseng, "Counterdiabatic mode-evolution based coupled-waveguide devices," Opt. Express **21**, 21224-21235 (2013).
19. S.-Y. Tseng and Y.-W. Jhang, "Fast and robust beam coupling in a three waveguide directional coupler," IEEE Photon. Technol. Lett. **25**, 2478-2481 (2013).
20. C.-S. Yeih, H.-X. Cao, and S.-Y. Tseng, "Shortcut to mode conversion via level crossing in engineered multimode waveguides," IEEE Photon. Technol. Lett. **26**, 123-126 (2014).
21. K.-H. Chien, C.-S. Yeih, and S.-Y. Tseng, "Mode conversion/splitting in multimode waveguides based on invariant engineering," J. Lightw. Technol. **31**, 3387-3394 (2013).
22. X. Chen, E. Torrontegui, and J. G. Muga, "Lewis-Riesenfeld invariants and transitionless quantum driving," Phys. Rev. A **83,** 062116 (2011).
23. X. Chen and J. G. Muga, "Engineering of fast population transfer in three-level systems," Phys. Rev. A **86**, 033405 (2012).
24. S. Martínez-Garaot, E. Torrontegui, X. Chen, M. Modugno, D. D. Guéry-Odelin, S.-Y. Tseng, and J. G. Muga, "Vibrational mode multiplexing of ultracold atoms," Phys. Rev. Lett. **111**, 213001 (2013).
25. H. R. Lewis and W. B. Riesenfeld, "An exact quantum theory of the time-dependent harmonic oscillator and of a charged particle in a time-dependent electromagnetic field," J. Math. Phys. **10,** 1458-1473 (1969).